Astron. Astrophys. 246, 587–596 (1991)

ASTRONOMY AND ASTROPHYSICS

The relationship between low-frequency oscillations in the chromosphere and background magnetic fields

V.E. Merkulenko and V.I. Polyakov

SibIZMIR, P.O. Box 4026, SU-664033 Irkutsk-33, USSR

Received May 14, accepted November 28, 1990

Abstract. Based on results of two-day observations in the wings of the Hα-line it has been established that:

(a) there exist in the chromosphere low-frequency oscillations, whose periods are close to those of the solar limb (Brown et al. 1978) as well as of coronal loops in soft X-rays (Harrison 1987).

(b) The wavelength of these oscillations is 600–700 Mm and is comparable with the scale of background magnetic field in the direction parallel to the equator.

(c) The amplitude of low-frequency oscillations is enhanced substantially at filament sites.

Key words: chromosphere – low-frequency oscillations – background magnetic fields

1. Introduction

We shall treat oscillations with periods over five minutes as low-frequency oscillations in the chromosphere. Information on these oscillations in the photosphere may be found in Deubner (1972), Stix & Wöhl (1974), Fossat & Ricort (1973), Merkulenko (1989); in the chromosphere (see Orall 1966; Sawyer 1974; Chipman 1977; Elliot 1969; Dame et al. 1984; Main 1977; Merkulenko & Mishina 1985; Merkulenko et al. 1988; Kneer & Uexkull 1983, 1985); in prominences (see Bashkirtsev & Mashnich 1984); in coronal loops observed in soft X-rays on SMM (see Harrison 1987); and in the radio range (see Kaufman 1972; Kobrin & Korshunov 1972). A wide spectrum of low-frequency oscillations of the outer solar limb was observed in papers by Hill's group (Hill et al. 1975; Brown et al. 1978). Low-frequency oscillations were identified with G-modes for $l = 1, 2$ by Delache et al. (1983) and Isaak et al. (1984). Oscillations with a period of 160 min should be specially separated (Severny et al. 1976; Brookes et al. 1976).

The observed oscillations with periods smaller than 35–40 min may be attributed to P-modes. According to calculations made by Dzembovsky & Pamjatnykh (1978), the G-mode amplitude can be comparable with the P-mode amplitude only for waves having a spherical harmonic $l = 2, 3$ and decreases six orders of magnitude if $l \geqq 15$ ($\lambda \leqq 300$ Mm), or can be tenths of cm s^{-1}. This value is significantly lower than the sensitivity of modern detectors. In this connnection, the observed oscillations with a period over 40 min, except for full-disk data when $l = 1, 3$, cannot be ascribed to G-modes. In this paper it will be shown that low-frequency oscillations which actually exist in the chromosphere, seem to be associated with dynamic processes in background magnetic fields.

Send offprint requests to: V.E. Merkulenko

2. Observational data and processing

The observations to be examined here include a sequence of filtergrams taken of the full solar disk in the wings of Hα ± 0.5 Å during two days in the time interval from 2^h18^m to 9^h30^m UT on 6 July 1988 and from 0^h14^m to 7^h56^m UT on 7 July 1988. Sequences of two frames in the opposite wings of Hα follow at intervals of 2 min. A Halle birefringent filter with the transmission band of 0.5 Å was used. The solar image was 51 mm in diameter. The resulution of the filtergrams is 2.0–2.″5 for 6 July 1988 and 1.5–2.″0 for 7 July 1988. Three photometric sections were made on each filtergram. One was made along the equator, and the other two were parallel at latitudes ±28°. These sections are marked by dashed lines on the filtergram for the Hα-line center for 7 July 1988 (Fig. 1). For the two observing days the initial point, when photometered, was tied to the same object in the neighbourhood of the active region NOAA 5061. The microphotometer slit is 5″ × 5″. As a result, we obtained six matrices of optical densities of the size 189 × 273 elements for 6 July 1988 which, with the projection effect taken into account, correspond to a scale of 1100 Mm and to the time interval of 432.2 min, and six 201 × 289 element matrices for 7 July 1988 with a scale of 1154 Mm and the time interval of 462 min. All in all, 658116 numbers if initial data were used for the entire processing.

The following operations were made for every matrix:

a) Conversion into intensities and division by the background, i.e., by the value of mean brightness along the photometric section.

b) Subtraction of the parabolic trend determined along the section.

c) Division by rms deviation of the variation of relative brightness along the section.

d) Determination, using two matrices, of relative values of brightness in the opposite wings of Hα of the matrices of the semi-sum and semi-difference.

$$B = (I^R + I^V)/2 \qquad V = (I^R - I^V)/2 \tag{1}$$

The variation of values of B and V must correspond to brightness and velocity oscillations, i.e., must give a similar spectrum. For clearness, it should be pointed out that operations

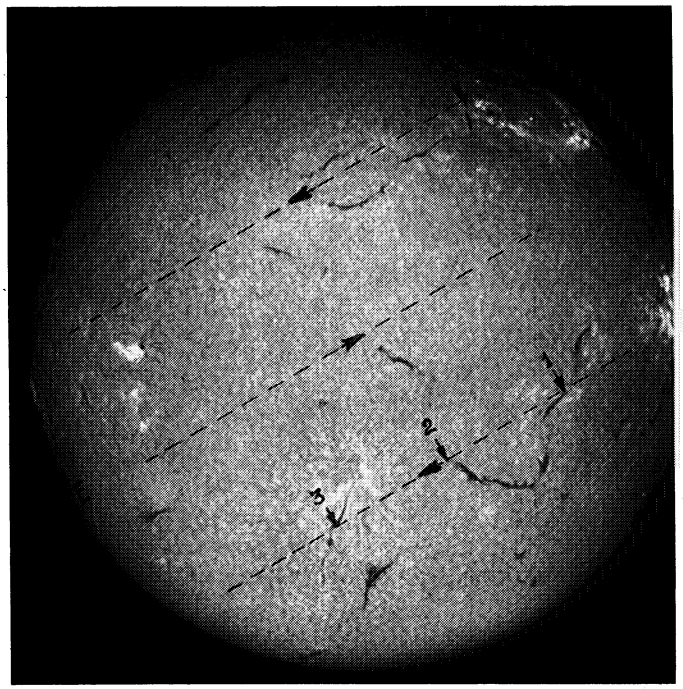

Fig. 1. The filtergrams taken at the Hα-line center on 7 July 1988. Dashed lines denote the photometric sections at latitudes 28° N, 0° and 28° S. The arrows indicate the filaments cut by the sections

"a–c" are performed separately for each filtergram. The purpose of such a processing is to reduce the influence of errors introduced by inaccurate exposure, changes in transparency of the Earth's atmosphere and in image quality, by the nonuniformity of illumination over the frame field due to limb darkening, etc. It is virtually impossible to determine exactly the influence of these errors. In the long run, a criterion for the correctness of the technique used is the repeatability of the final results for the two observing days, proved that there is a large statistics of initial data.

3. Two-dimensional spectral analysis of the velocity and brightness oscillations in the Hα-line

The spectra were calculated by the method of two-dimensional correloperiodogram analysis (CPGA-2). This technique implies determining the multiple correlation coefficient between an initial two-dimensional series $L(x,t)$ and the values of $C(x,t)=\cos(\omega t-kx)$ and $S(x,t)=\sin(\omega t-kx)$ (Hannan 1960; Kopecky & Kuklin 1971). The regression equation for these quantities may be written as:

$$L-\bar{L}=A(C-\bar{C})+B(S-\bar{S}) \qquad (2)$$

where

$$A=(\overline{LC}-\bar{L}\,\bar{C})/(\overline{C^2}-\bar{C}^2) \qquad B=(\overline{LS}-\bar{L}\,\bar{S})/(\overline{S^2}-\bar{S}^2)$$

are the partial regression coefficients. The overscribed bar corresponds to the operation of determininga mean.

By specifying different values of the period $T=2\pi/\omega$ and wavelengths $\lambda=2\pi/k$, one can find two-dimensional functions of the amplitude of these harmonics

$$P(\lambda,T)=(A^2+B^2)^{1/2} \qquad (3)$$

or the multiple correlation coefficient

$$\varrho(\lambda,T)=P(\lambda,T)/(\overline{L^2}-\bar{L}^2)^{1/2}. \qquad (4$$

The CPGA-2 method is convenient for determining periods anc wavelengths comparable with the realization length. It "works' for data with a variable step of argument. The disadvantage of thi method is that the computer time consumed is considerable. Fo the same realization, the position of maxima on periodograms fo $P(\lambda,I)$ and $\varrho(\lambda,T)$ coincides; at the same time the quantity $P^2(\lambda,T)$ can be regarded as an analog of spectral density of the Fourier distribution. In this connection, in this paper wher making a spectral analysis, we have determined the functior $P(\lambda,T)$. For three photometric sections and for the two observing days, we have calculated six two-dimensional spectra of velocity V and six spectra of brightness B. After that, separately for V and B averaging was done over four spectra for latitudes ±28 (Fig. 2a, b), and over two spectra on the equator (Fig. 3a, b), i.e. the spectra were averaged over two observing days. Besides, ir order to determine global pulsations in the chromosphere, we determined a mean for all of the six matrices for V and six matrices for B (Fig. 4a, b). On each spectrum the abscissa axis indicates the wavelength in Mm, and the axis of ordinates indicates the period T in minutes. A step in the spectrum is 1 min for periods in the interval from 2 to 100 min and is 2 min in the interval from 100 to 250 min. For wavelengths, it is 20 Mm. The isolines follow at intervals of 0.1 from the spectrum maximum, and the last ninetl isoline corresponds to values of $P(\lambda,T)$ which on all spectra exceed the confidence interval level of 0.90. On the averaged spectrum for V and B (Fig. 4a, b), the maximum of the brightness spectrum is 7.5 times larger than that of the velocity spectrum.

Let us examine the main peculiarities of the spectra.

a) The main maxima of velocity and brightness oscillations correspond to the wavelength range 600–700 Mm.

b) In the low-frequency region the velocity oscillation amplitude at the equator exceeds that at latitudes $\pm28°$.

c) On the brightness oscillation spectra the maxima are displaced to the low-frequency region.

The first and second solumns in Table 1 give the periods and spectral amplitudes of velocity oscillations on the equator (Fig. 3a). The third and fourth columns list the periods and amplitudes at latitudes $\pm28°$ (Fig. 2a). The fifth and sixth columns present the periods and amplitudes on the averaged spectrum (Fig. 4a). The seventh column gives the periods of solar diameter oscillations according to the data reported by Hill's group (Brown et al. 1978). The eighth column presents the oscillation periods of coronal loops in soft X-rays (Harrison 1987).

Thus, the data listed in Table 1 induce us to conclude that the chromosphere supports low-frequency oscillations, whose periods are comparable with periods of solar diameter oscillations as well as of coronal loops in soft X-rays.

4. The relationship between the background magnetic field and low-frequency oscillations in the chromosphere

4.1. Spatial spectrum of the background magnetic field

In order to solve this problem, we have used synoptic maps of the magnetic field obtained at the Kitt Peak observatory for Carrington rotation 1804 (12 July–29 July 1988) published in Solar Geophys. Data (1988). Two maps corresponding to the distribution of the magnitude and polarities of the field were copied on

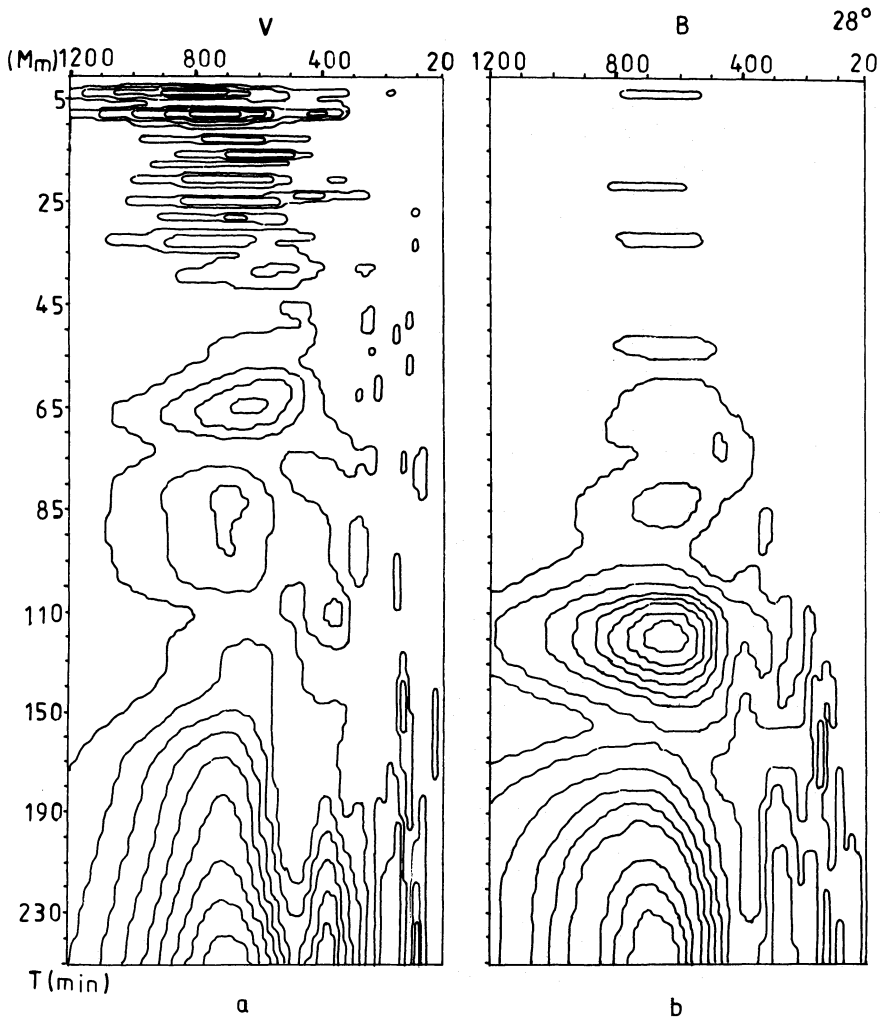

Fig. 2a and b. Two-dimensional averaged spectra $P(\lambda, T)$ of velocity V and brightness B for latitudes $\pm 28°$. The CPGA-2 method has been used in the calculations. The isolines follow at intervals of 0.1 from the spectrum maximum. **a** Averaged spectrum of velocity V for latitudes $\pm 28°$ for two observing days. **b** Averaged spectrum of brightness B for latitudes $\pm 28°$ for two observing days

able 1. Observed and calculated periods (min)

$=0°$		$\varphi = \pm 28°$		Averaged		Brown et al. (1978)	Harrison (1987)	$T_n = T_0/n$	
	P	T	P	T	P	T	T	n	T_n
								1	193
)0	1.0	85	0.3	96	0.5	105	94	2	96
58	0.5	66	0.4	66	0.4	66	68	3	64
47	0.8			46	0.2	45	45	4	48
38	0.3	39	0.2	38	0.2	39		5	39
34	0.4	33	0.2						
31	0.3			32	0.2			6	32
27	0.5	28	0.2	28	0.2	29		7	27
25	0.4	25	0.2	25	0.3	25	24	8	24
21	0.3	21	0.2	21	0.2	21		9	21

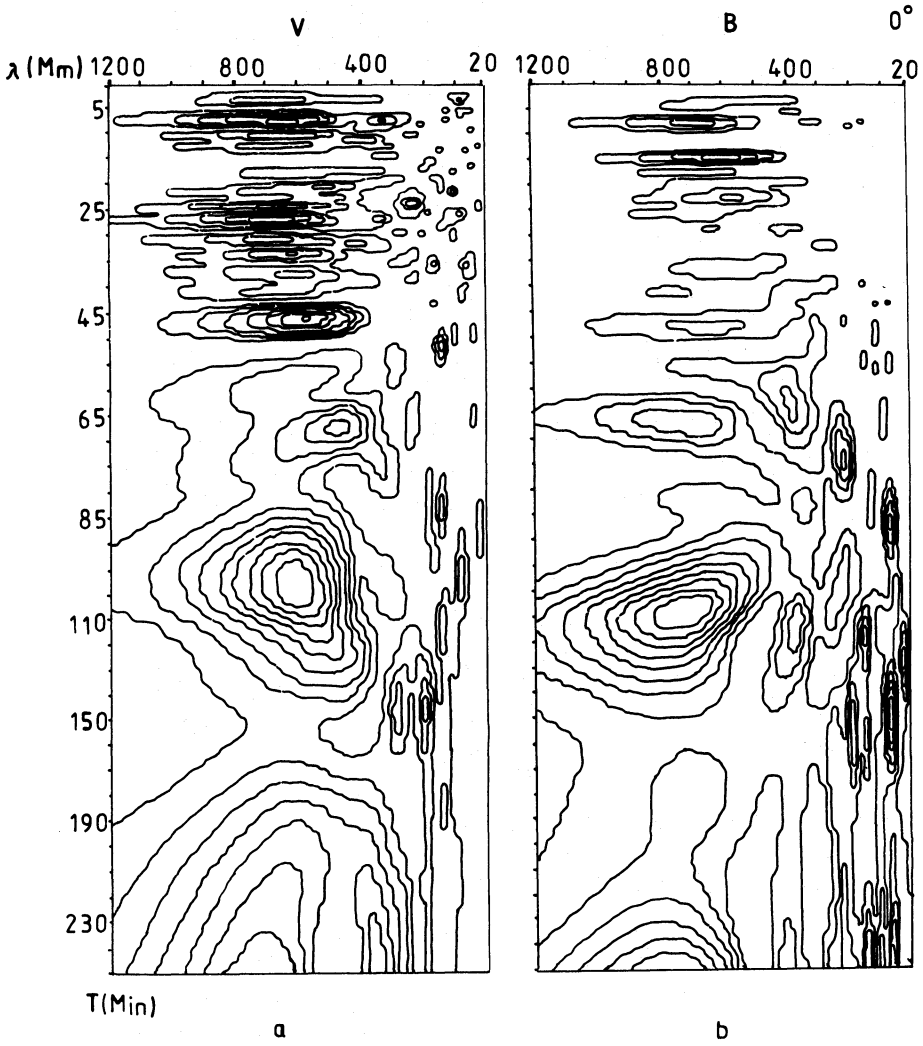

Fig. 3a and b. Same as Fig. 2 but for the equator

a photoplate. Photometering was carried out in longitude, from zero to 360° along the equator as well as at latitudes 28° N and 28° S, with the number of points along the section equal to 385. Photometering data were then used to make a spectral analysis by the method of one-dimensional CPGA. The result is presented in Fig. 5 where the abscissa axis indicates the wavelength λ in Mm, and the axis of ordinates indicates the amplitude $P(\lambda)$. The dashed horizontal line corresponds to the level of the 0.90 confidence interval. The solid curve denotes the spectrum of the distribution in space of the field polarity, and the dashed curve indicates the magnitude of the field. One can see that on the spectra for 28° N and 28° S the main maximum corresponds to 620 Mm, and that on the spectra for the equator corresponds to 700 Mm. Thus, for sections parallel to the equator, areas with the same polarity of the background magnetic field are separated at a distance of 600–700 Mm, on the average. By comparing the two-dimensional oscillation spectra in Figs. 2–4 with the spatial spectrum in Fig. 5, it may be concluded that in the direction parallel to the equator the wavelength λ of low-frequency oscillations is comparable with the scale of the spatial distribution of the background magnetic field.

4.2. Enhancement of the amplitude of low-frequency oscillations at the location of filaments

Let us consider the variation of the oscillation amplitude along th photometric sections portrayed in Fig. 1. Let us separate th periods of 24, 45, 68, and 94 min, to which oscillation maxima c coronal loops in soft X-rays correspond (Harrison 1987) and let u add to them the 160 min period. For these periods, we sha determine the variation in amplitude of the spectrum $P(L, T$ along the photometric sections. The results of the calculation ar presented in Fig. 6a for the section at latitude 28° N, in Fig. 6b fo 0°, and in Fig. 6c for 28° S. The abscissa axis indicates distance in Mm, and the axis of ordinates indicates the amplitude c spectrum P normalized to the maximum which is taken the sam for all spectra. The right-hand part of the plots indicates the valu of the period, for which the spectrum is calculated. The upper tw sequences of spectra correspond to velocity V, and the lower one correspond to brightness B. The date of the observation is marke in the left-hand part of the plots. At bottom, one can see the profil of the background magnetic field distribution constructed on th

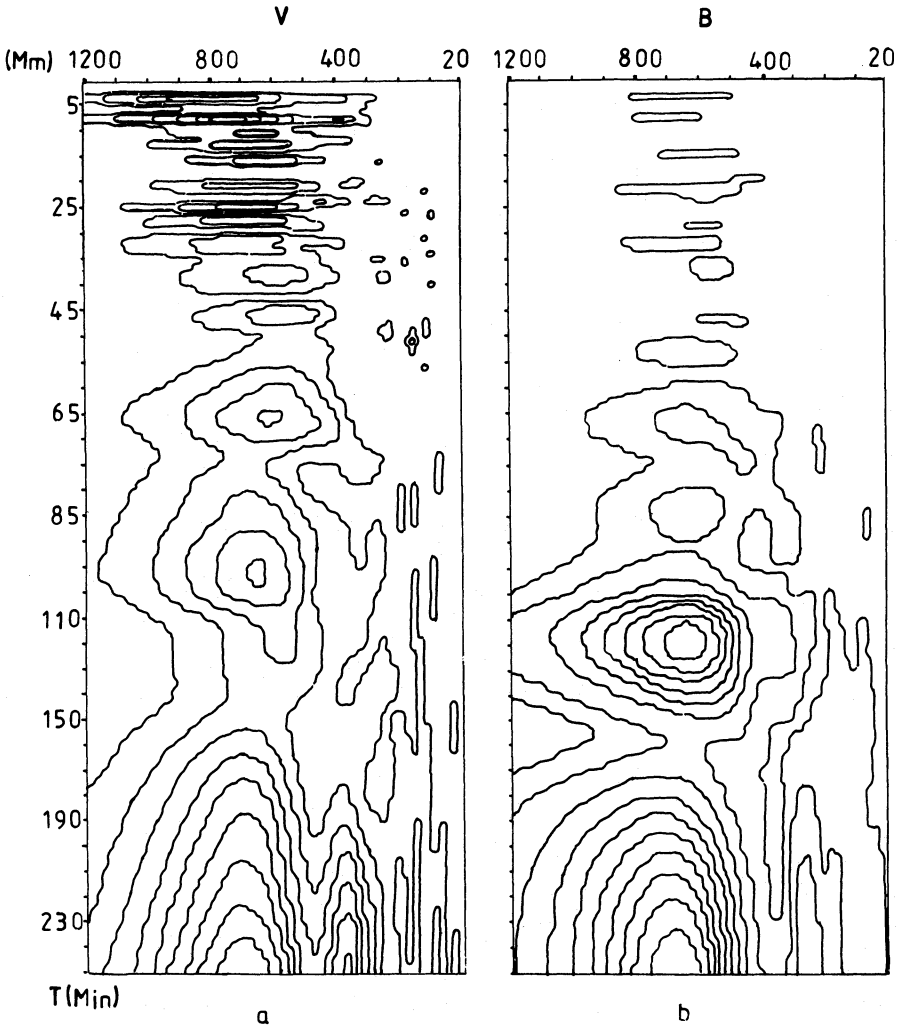

Fig. 4a and b. Two-dimensional averaged velocity and brightness spectra for latitudes ±28° and for the equator for two observing days. **a** Averaged velocity spectrum. **b** Averaged brightness spectrum

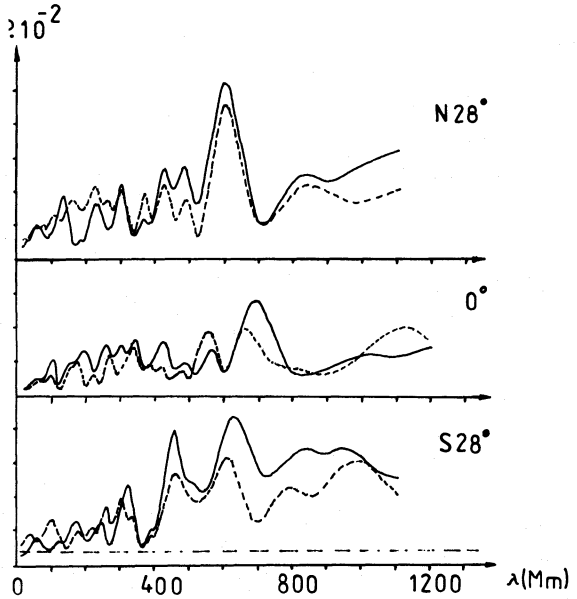

g. 5. Spatial spectra of the background magnetic field from synoptic maps of arrington rotation 1804. Photometric sections are made from 0 to 360° at titudes 28° N, 0°, 28° S. The solid curve denotes the polarity distribution ıectrum; the dashed curve shows the distribution spectrum of the magnitude of ɛld

basis of the data of photometering the synoptic maps along the photometric sections marked in Fig. 1. The solid curve corresponds to the map of field polarity distribution, and the dashed curve corresponds to its amplitude distribution.

In Fig. 6a–c one can see that in some regions of sections for both the first and second observing days, there occurs a significant increase in spectrum amplitude which covers the entire range of periods from 24 to 160 min and manifests itself for both the brightness and the velocity. The filtergram in Fig. 1 suggests that areas with enhanced oscillation amplitude correspond to intersections of the photometric sections with individual filaments. One such intersection occurrec for the 28° N section, and three intersections occurred for 28° S. The position of the filaments in Figs. 6a and 6c is indicated by vertical dashed lines as well as by the arrows in Fig. 1. As one would expect, these areas are located, with respect to the backbround magnetic field, near the neutral line. On the equator, the section does not intersect the filaments. As a consequence, Fig. 6b is lacking areas of increased amplitude which could cover the entrire spectrum interval. One some occasions there is an enhancement of the oscillation amplitude on the periods 94–160 min. It should be noted that the spectrum maximum does not always correspond exactly to the point of intersection of the section with the filament, having a transverse size of about 7″. Thus, for the observations of 6 July 1988 (Fig. 6c) on the spectrum for V, it is displaced with respect to the filament by 30″. For this same observing day on the spectrum for B of the

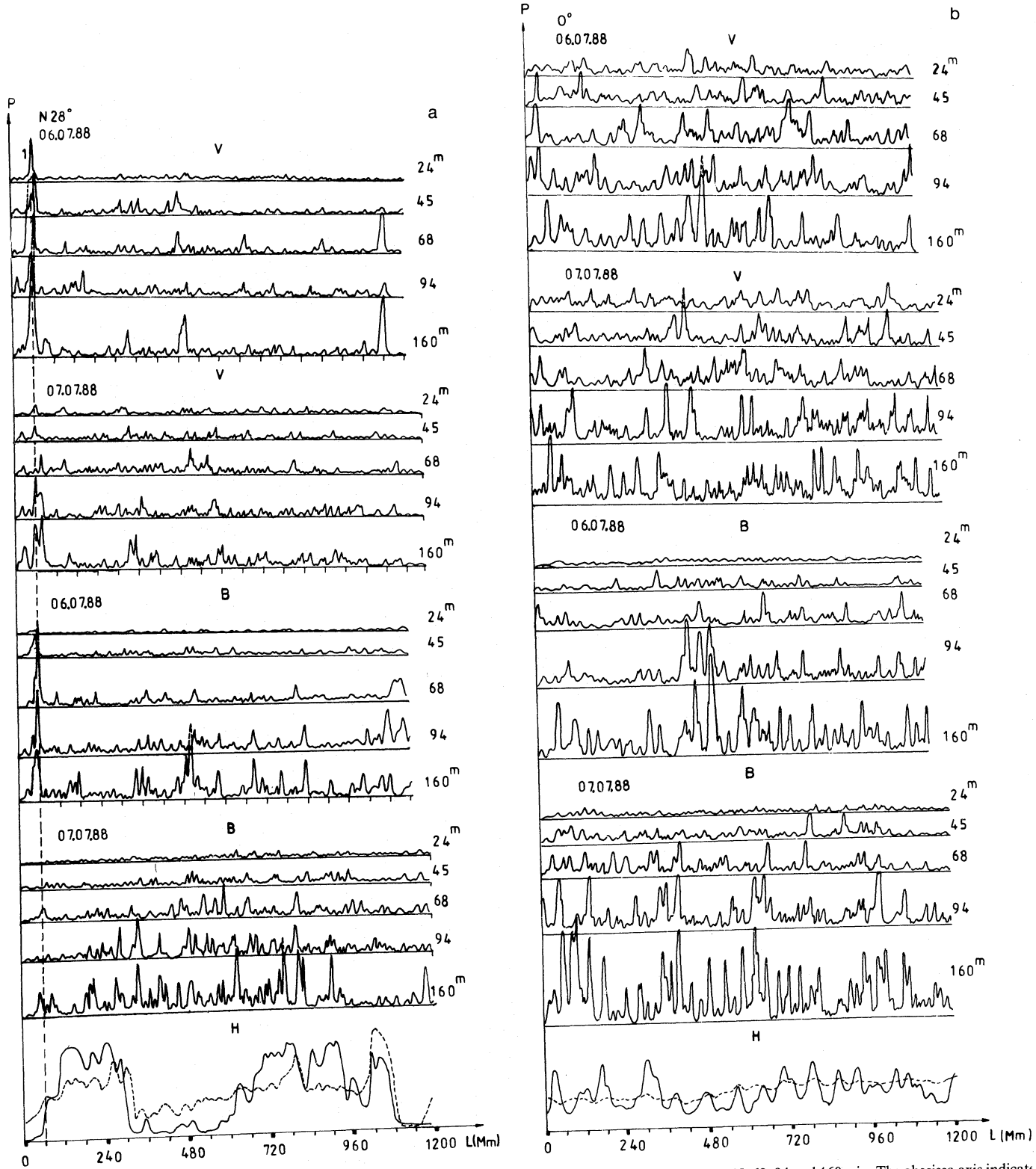

Fig. 6a–c. The distribution of the spectrum amplitude along photometric sections for the selected periods of 24, 45, 68, 94 and 160 min. The abscissa axis indicate the distance in Mm, and the axis of ordinates indicates the spectrum amplitude. The date of the observation is marked in the left-hand part of the plots. The upper tw sequences correspond to the velocity, and the lower ones refer to the brightness. At the bottom of the plots, one can see the distribution of the background magnet field along the section on the basis of data of photometering the synoptic maps. The solid line corresponds to the polarity distribution map, and the dashed line refe to that of the magnitude of field. Dashed vertical lines denote the position of the filaments which are traversed by photometric sections. **a** Spectra for the section i latitude 28° N. **b** Same but for the equator. **c** Same but for latitude 28° S

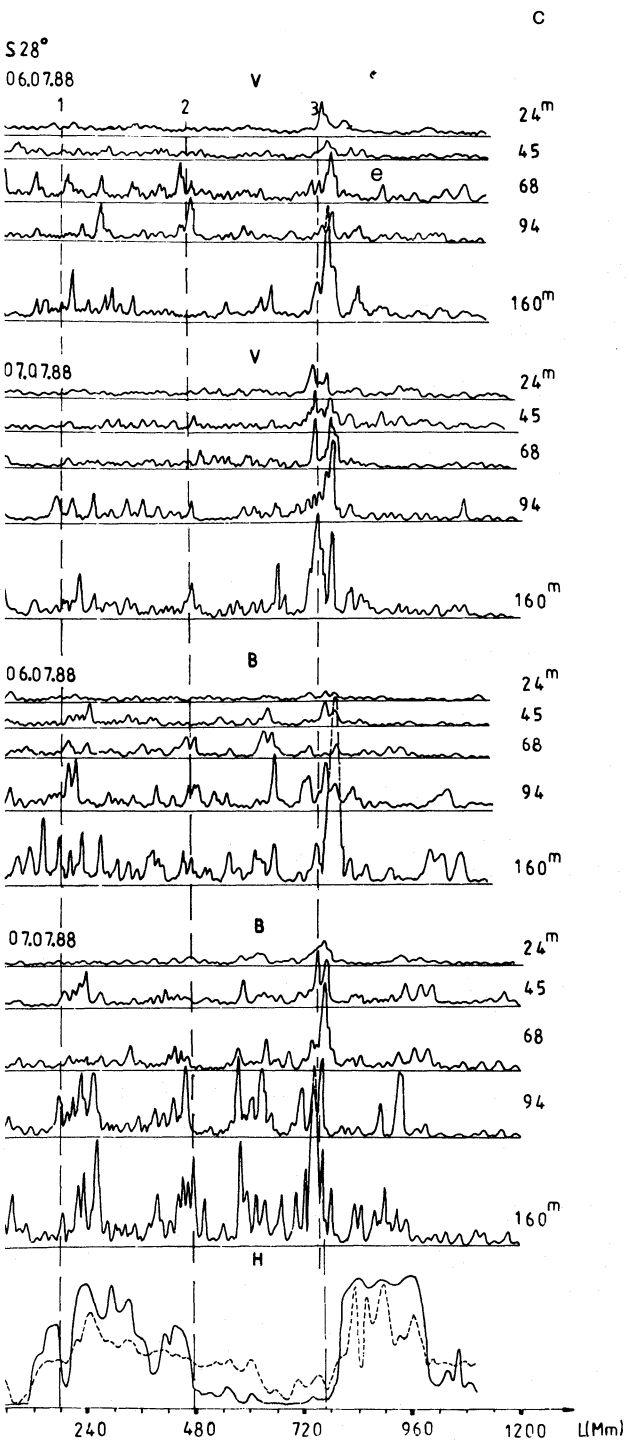

. 6 (continued)

160 min period, it is displaced by 35″. Unlike filament "3", the spectra in the vicinity of filaments "1" and "2" are more blurred. As follows from Fig. 1, for filament "1" this is associated with the fact that at a significant distance the photometric section coincides with its direction as a consequence of the broken bend of the trajectory. Filament "2" does not intersect the section but only makes contact with its extreme point. Between filaments "1" and "3" and filament "2", there is an important difference. Thus, while the former ones are the separation boundary of bipolar structure of global background magnetic fields which are elongated at an angle of 25–30° equatorward, filament "2" is oriented at an angle of 120° and seems to be located inside of the bipolar structure.

On the basis of the data obtained one can suppose that regions of localization of the filaments are antinodes for waves, whose spectra are presented in Figs. 2–4. Obviously, for $\lambda_0 = 600$ Mm, the antinodes will be separated by 300 Mm, i.e., at a distance between two neighbouring filaments shown in Fig. 6c. It should be noted that in the processing of the data we have eliminated the parabolic trend along the photometric section, thereby filtering out the oscillations, whose wavelength is comparable with the scale of the realization. As a consequence of this, it is possible that a harmonic exists, for which $\lambda = 2\lambda_0 = 1200$ Mm (Merkulenko et al. 1988).

5. Discussion

5.1. *Instrumental and seeing effects*

The main possible nonsolar effects which may produce maxima in the power spectra in Figs. 2–4, are: periodic changes of the value of mean brightness along the photometric section as well as in contrast due to seeing or the value of rms deviation of the variation of relative brightness along the section.

In Fig. 7 curves 1–11 and 14–24 represent, in the neighbourhood of filament "3", the time variation of V defined by Eq. (1). Column "a" corresponds to the observations on 6 July, and column "b" corresponds to those obtained on 7 July 1983. Each curve determines areas of the size 5″ × 5″ on the time interval over 420 min. Visually, one can identify the low-frequency component of the oscillations on curves 6 and 19 which corresponds to the area covered by the filament. Curves 13 and 26 represent the time variation of the value of the semi-sum, F, of mean brightnesses of the section 28° S of the red and blue wings of the Hα-filtergram. Curves 12 and 25 correspond to the variation in contrast of the semi-difference, S, of rms deviation of relative brightness of the red and blue wings along this section.

Figure 8a, b present the oscillation spectra of V for curves 6 and 19, and Fig. 8c, d gives spectra F for curves 13 and 26, and Fig. 8e, f shows spectra S for curves 12 and 25. The spectra were calculated by the method of one-dimensional CPGA. The abscissa axis indicates the period in the interval from 6 to 255 min. The axis of ordinates indicates amplitude P normalized to the maximum which is taken the same for all of these spectra. One can see that on the spectra for F(Fig. 8c, d) the low-frequency component is virtually absent. As far as the rapid pulsations on curves 13 and 26 are concerned, they are caused by a systematic instrumental error of the exposure time. With the interval between the sequences of two minutes, this can give on the spectrum a spurious peak on a period of 4 min; however, in accordance with the Nyquist's criterion there is no point in considering it here. Curves 12 and 25 for contrast S deserve more serious attention; they clearly show a low-frequency component. At the same time, by comparing curve

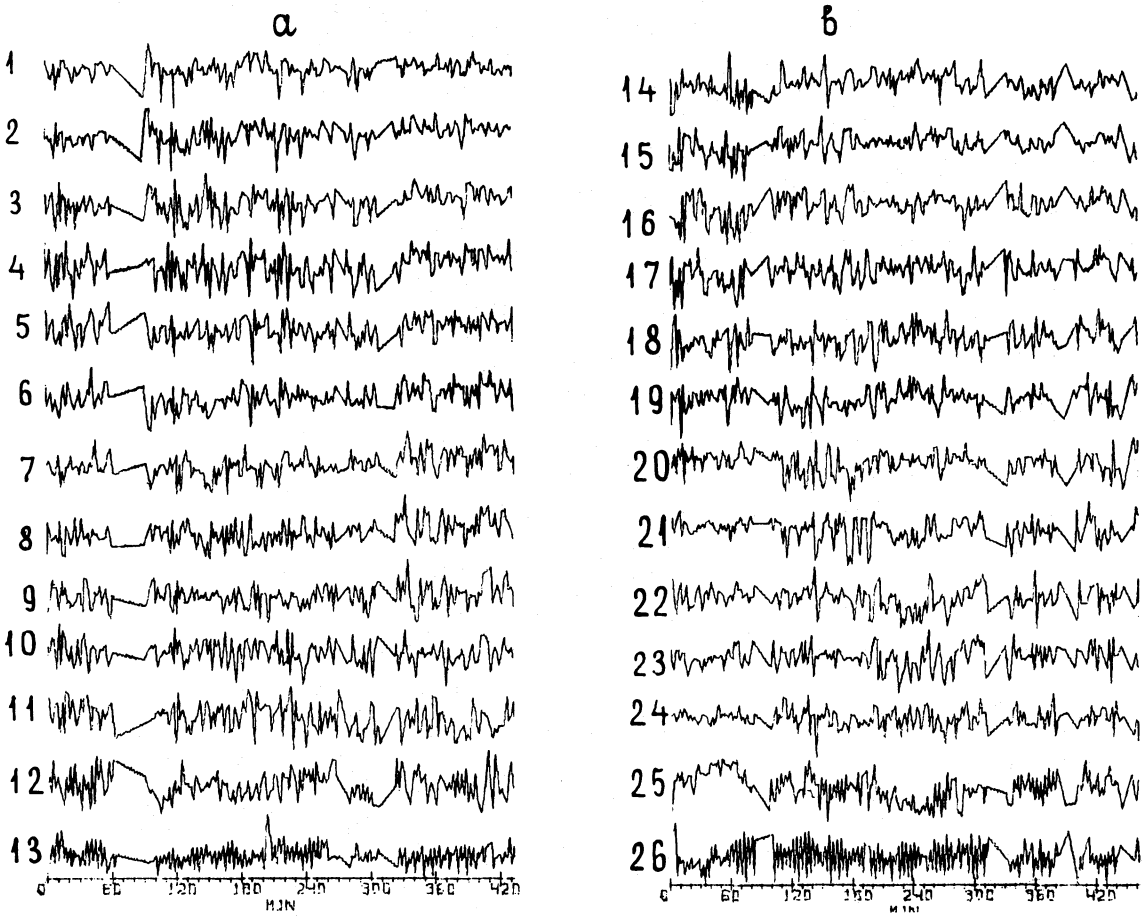

Fig. 7a and b. Velocity oscillations in the neighbourhood of filament "3" of section 28° S. A 5″ × 5″ area corresponds to each curve. **a** Observations of 6 July, and observations of 7 July 1988. Curves 6 and 19 correspond to filament oscillations, curves 13 and 26 refer to the variations of the semi-sum, *F*, of mean brightness along the section for the blue and red wings, and curves 12 and 25 represent the variations of the semi-difference, *S*, of rms. deviations of brightness along this secti

19 for filament oscillations with curve 25 for *S*-oscillations, one can note that the phases of these curves do not coincide. Besides, there exists an obvious difference in the spectra of the filament oscillations (Fig. 8a, b) and in the spectra of contrast *S* (Fig. 8e, f).

Figure 8g, h presents the averaged spectra of *S* and *F* for sections along the equator for two observing days. Figure 8i, j gives the result of a similar averaging over latitudes ±28°, and Fig. 8k, l presents the spectra of these values averaged over the three photometric sections for two observing days. By comparing these spectra with the averaged two-dimensional spectra in Figs. 2–4, one should note their marked lack of coincidence on the position of the peaks along coordinate *T*, which suggests the reality of the existence of low-frequency oscillations in the chromosphere. It is also possible, however, that the peak for the period of 105 min identifiable on the spectra in Fig. 8g, i, k for contrast *S* is the response of the terrestrial atmosphere to the corresponding period of the oscillations in the solar atmosphere.

5.2. *The interpretation of the low-frequency oscillations*

In accordance with the data of the synoptic maps in the latitude range ±60°, the structure of the background magnetic field can, probably, be represented as a set of parallel magnetic ropes located horizontally along the solar surface and elongated by tl differential rotation along the equator at an angle of 25–30°. If it assumed that the outer envelope of each rope consists of tl toroidal component, then – as a consequence of their incomple emergence above the photosphere – this component on synopt maps must be manifested as the longitudinal component of tl background magnetic field. According to the spectral distributic of this field in space (Fig. 5), the transverse scale of such a ro must be $l_0 = \sin 30° \times 600\,\text{Mm} = 300\,\text{Mm}$. Based on the equili rium and stability condition, it should be anticipated that tl central part of each rope consists of the poloidal component. A the magnetograph sensitivity is increased, this component ca perhaps, be observed as the transverse component of the bac ground magnetic field. Above the photospheric level, on the line contact of the neighbouring ropes, a neutral sheet, i.e., tl reconnection region of the toroidal component of the magnet field must be produced. As a result, magnetic loops, with the convexity downward, which are produced above the neutral lin are able to sustain the cold dense plasma of the filament formed a consequence of a thermal instability. A scheme for suc reconnection is presented in Fig. 9. The photospheric level coi cides with axis *X*. Cross-section areas of the filament are shade The arrows indicate the direction of the field lines of the toroid and poloidal components. A chain of forming filaments must l located at an angle of 25–30° symmetric about the equator at

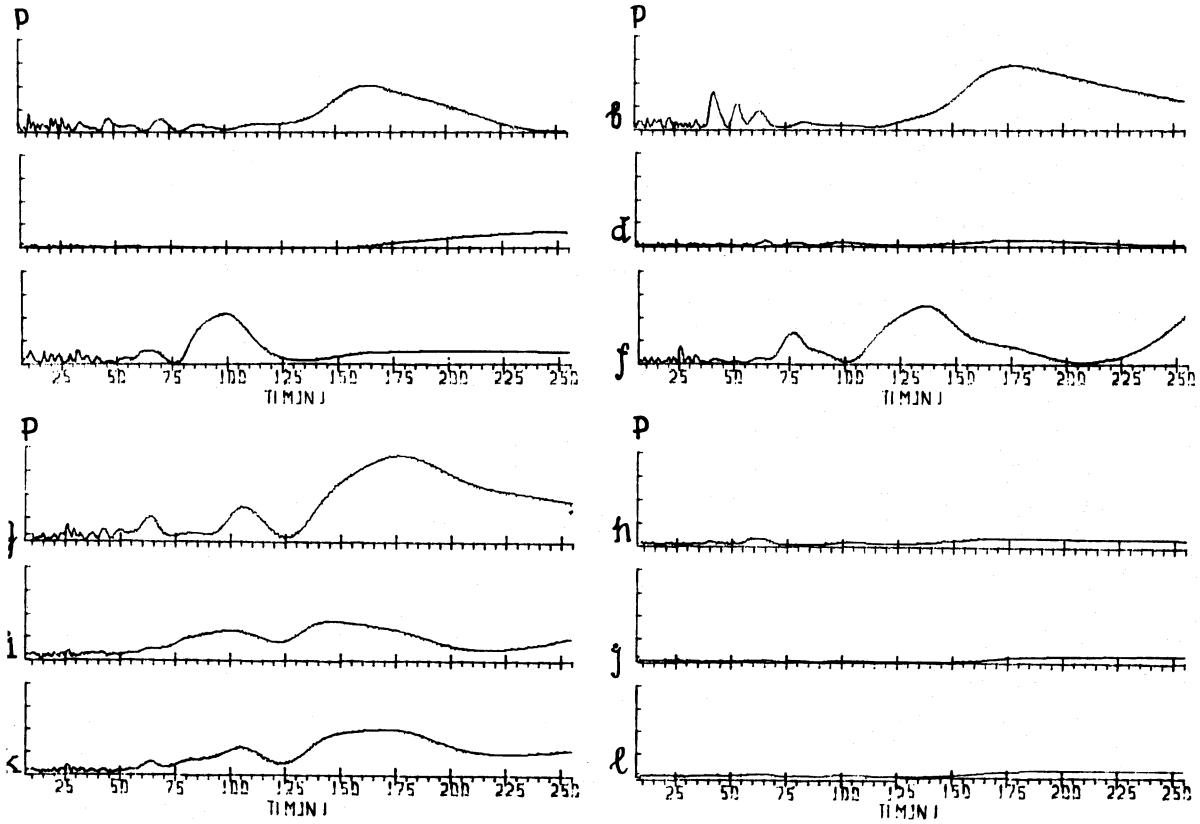

g. 8a–l. One-dimensional CPGA spectra: **a** for curve 6 in Fig. 7, **b** for curve 19, **c** for curve 13, **d** for curve 25, **e** for curve 12, **f** for curve 25, **g** for mean values of S for 28° sections for two observing days, **h** same but for F, **i** for mean values of S for sections along the equator, and **j** same but for F, **k** for mean values of S for all ctions for two observing days, and **l** same for F

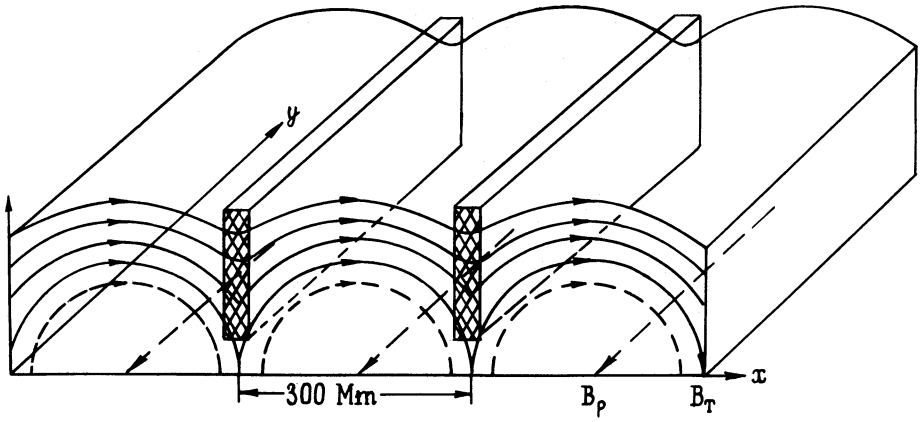

Fig. 9. A possible scheme for the structure of the background magnetic field in the form of horizontal magnetic ropes. The toroidal component of the ropes is observed as the longitudinal component on the synoptic maps. The filaments are located on the boundary of contact made by neighbouring ropes. They are sustained by magnetic field loops produced due to reconnection of the toroidal component

istance of 600–700 Mm in the cross-section parallel to the quator.

According to the calculations made by Kuperus & Raadu 1974), a filament in the gravitational field can perform oscil-ıtions with period $T = 2\pi (h/g)^{1/2}$, where h is the height of the lament, g is acceleration of gravity. For a typical filament, $= 5\ 10^9$ cm. Hence $T = 45$ min. This period can, perhaps, be egarded as the fundamental harmonic of the prominence oscil-ıtions. Alternatively, in accordance with the scheme in Fig. 9, the ıagnetic fields sustaining the filament must renonnect through ıe corona in the form of loops. Oscillation periods of these loops an be estimated from the expression $T_n = 2l(4\pi\varrho_i)^{1/2}/n B_i$, where l is the loop length, ϱ_i is plasma density inside the loop, and B_i is the field strength. According to the data reported by Priest (1978), in a quiet region, loops observed in soft X-rays have a density of $2\ 10^{-16}$–10^{-15} g cm^{-3} and a length of 20–700 Mm. Taking $l = \pi l_0/2 = 470$ mm for $\varrho_i = 3\ 10^{-16}$ g cm^{-3} and $B_i = 0.5$ G we find $T_1 = 193$ min. The spectrum of values of T_n is presented in column 10 of Table 1. By comparing these periods with the observational data, one can suppose that coronal magnetic structures may, in principle, give rise to a resonance excitation of oscillations at low frequencies. In this connection, there arises the question of the energy source for such oscillations. As shown by Dzembovsky & Pamjatnykh (1978), gravity waves in the tran-

sition region pass into the class of surface waves and do, virutally, not reach the photosphere. It remains to suppose that, as the response to the G-mode oscillations, a disturbance in the form of Alfven waves propagate from the base of the convection zone along the magnetic field. Indeed, according to the data reported by Stix & Wöhl (1974) as well as by Deubner (1972), the wave amplitude with a period of 20–50 min grows from disk center to limb, i.e., these waves are tangential rather than radial ones. In accordance with the scheme in Fig. 9, the magnetic field must pierce the entire convection region, and its concentration is substantially enhanced at sites of the filaments. Thus, the filaments should, presumably, be viewed as sources of low-frequency oscillations in the solar atmosphere, and the identified periods of these oscillations seem to be associated with resonant properties of the background magnetic field. With such an approach, it is no longer appropriate to identify the observed periods with G-modes of the global pulsations of the Sun; however, this provides new possibilities of investigating the physical conditions in coronal magnetic structures.

6. The main conclusions

Let us summarize the main conclusions of this paper.

a) The chromosphere exhibits low-frequency oscillations with periods of 96, 66, 46, 38, 32, 28, 25, and 21 min.

b) The wavelength of these oscillations is 600–700 Mm and is comparable with the scale of the background magnetic field in the direction parallel to the equator.

c) The amplitude of low-frequency oscillations is substantially enhanced in the region of filaments.

Acknowledgements. We are indebted to Prof. P. Mein for helpful suggestions which helped to improve our paper. Special thanks are due to Mr. V.G. Mikhalkovsky for his assistance in preparing the English version of the manuscript and for typing and retyping the text.

References

Bashkirtsev V.S., Mashnich G.P., 1984, Solar Phys. 91, 93
Brookes J.R., Isaak G.R., van der Raay H.B., 1976, Nat 259,
Brown T.M., Stebbins R.T., Hill H.A., 1978, ApJ 223, 324
Chipman E.Q., 1977, Solar Phys. 55, 277
Dame L., Goutebroze P., Malherbe J.M., 1984, A&A 130, 33
Delache P., Scherrer P.H., 1983, Nat 306, 651
Deubner F.-L., 1972, Solar Phys. 22, 263
Dzembovsky W., Pamjatnykh A.A., 1978, Deuxieme Assemb Europienne de Physique Solaire, ed. J. Rosch, Paris, CNRS, 135
Elliot J., 1969, Solar Phys. 61, No. 1, 28
Fossat E., Ricort G., 1973, Solar Phys. 28, 311
Hannan E.J., 1960, Time Series Analysis. Methuen, London, Ne York, Wiley, New York
Harrison R.A., 1987, A&A 182, 337
Hill H.A., Stebbins R.T., 1975, ApJ 200, 471
Isaak G.R., van der Raay H.B., Pall P.L., Roca Cortres Delache P., 1984, Mem. Soc. Astron. Ital. 55, 99
Kaufmann P., 1972, Solar Phys. 23, 178
Kobrin M.M., Korshunov A.I., 1972, Solar Phys. 25, 339
Kopecky M., Kuklin G.V., 1971, in: Issledovaniya po geomagne izmu, aeronomii i fizike Solntsa, Irkutsk 2, 167
Mein N., 1977, Solar Phys. 52, 283
Merkulenko V.E., Mishina M.N., 1985, A&A 146, L9
Merkulenko V.E., Mishina M.N., Yazev S.A., 1988, Ibid. 20 131
Merkulenko V.E., 1989, in: Issled. po geomagnetizmu, aeronom i fizike Solntsa 87, 171
Orall F.Q., 1966, ApJ 143, 917
Priest E.R., 1978, Solar Phys. 58, 57
Sawyer G., 1974, Solar Phys. 35, 61
Severny A.B., Kotov V.A., Tsap T.T., 1976, Nat 259, 87
Solar-Geophys, Data Prompt Reports, September 1988, No. 52 Pt. 1, Data for August and July 1988, NOAA
Stix M., Wöhl H., 1974, Solar Phys. 37, 65